Iranian Society of Acoustics and Vibration
The 9th ISAV2019 International Conference on Acoustics and Vibration
24-25 Dec 2019 Tehran - Iran
Iran University of Science & Technology

Energy Harvesting Using MEMS Porous Functionally Graded Piezoelectric Cantilever Beam

Easa AliAbbasi[a*], Akbar Allahverdizadeh[b], Behnam Dadashzadeh[b], Reza Jahangiri[c]

[a] *MSc, School of Engineering-Emerging Technologies, University of Tabriz, 29 Bahman Blvd, 5166614761, Tabriz, Iran.*

[b] *Assistant Professor, University of Tabriz, 29 Bahman Blvd, 5166614761, Tabriz, Iran.*

[c] *Assistant Professor, Islamic Azad University, Salmas Branch, Salmas, Iran.*

** Corresponding author e-mail: e.abbasi.edu@gmail.com*

Abstract

This study deals with the analytical design of a vibrational energy harvester which is composed of functionally graded piezoelectric material. The effects of porosity existence on the responses of the FG piezoelectric MEMS bimorph cantilever beam is investigated with both axial and transverse deformations. Furthermore, Hamilton's principle is utilized in order to obtain the governing equations of motion and also, they are solved by Galerkin method. Since the effect of elastic mode shapes related to lower frequencies are overcoming the higher frequencies mode shapes, some of the first mode shapes are utilized for studying the transverse shape changing of Euler-Bernoulli beam. Moreover, the frequency response is carried out for the case of near resonance frequencies due to the effects of volume fraction index and porosity coefficient with different values. The output power of the energy harvester is presented with respect to the output resistance in order to obtain the enhanced efficiency.

Keywords: piezoelectric; functionally graded materials; porosity; bimorph cantilever beam.

1. Introduction

During past decades, because of the wide range use of wireless sensors, vibrational energy harvesting has received significant attention. It is a green energy and almost available everywhere. Due to the environments and circumstances of wireless sensors, providing their required power for operation in the place would be appreciated. Though, piezoelectric cantilever beams are applied and

has many advantages over other transducers [1]. They are easy to apply without external power sources and also have high electromechanical coupling coefficient [2, 3]. In addition to that, these transducers could be used in different fields such as fire or gas detection, fault diagnosis and environmental monitoring [4, 5].

Most of the piezoelectric transducers operate near the natural frequency, but in some occasions, low frequency vibrations are initial. So, output power enhancement is required by improving the materials or the shape of the transducer [6]. Piezoceramics and piezoelectric polymers are the two classifications of homogeneous piezoelectric materials. The electromechanical coupling coefficient of piezoceramics are significantly greater than piezoelectric polymers. As an advantage, piezoelectric polymers are more flexible and endure high mechanical strain compared to the other one. Therefore, composite materials are fabricated as functionally graded materials (FGMs) to avoid stress concentration and crack propagation. They are advanced materials composed of different materials such as polymers, ceramics or metals in which, their properties vary over a specific spatial direction. In addition, FGPMs increase the durability of piezoelectric devices and produce larger displacements [7].

It was realized that during FGMs sintering process, voids of porosities could be created to affect stiffness and reliability of structures [8]. They were air bubbles entering the matrix material during melting or mixing processes and it was because of the difference in solidification temperatures of material constituents [9].

Porous FG piezoelectric cantilever beams are widely utilized in different scale ranges for energy harvesting. The thickness stretching and porosity effects of FG beams was presented by Atmane et al. The proposed beam was resting on an elastic foundation and using the Vavier technique, the closed form solutions were extracted [10]. Studying large amplitude vibrations of a porous Timoshenko beam, a power-law model was proposed by Ebrahimi and Zia. It was found that the increase in porosity, increases the ratio of nonlinear to linear resonant frequencies. Also, the mechanical parameters of the beam was described by the model [11]. By employing a semi-analytical differential transform method, thermo-mechanical vibrations of FG beams with porosities was studied by Ebrahimi and Jafari [12]. Furthermore, investigation of angular velocity effects on wave propagation of FG porous piezoelectric nanobeams was carried out by Ebrahimi and Dabbagh. It was concluded that, higher phase velocity, wave frequency and escape frequencies would be the result of higher porosity [13]. In addition, based on the modified couple stress and Euler-Bernoulli beam theories, vibrations of imperfect FG porous tapered microbeams was studied by Shafiei et al. [14].

Using first order shear deformation theory, together with Eringen's nonlocal elasticity theory, design and analysis of FG Timoshenko beam with non-uniform structure was presented by Lal and Dangi. Across the thickness, the beam was studied under linear and non-linear temperature profile [15]. In addition to that, prediction of the energy harvesting capabilities of a porous piezoelectric energy harvester was generated by Martinez-Ayuso et al. The estimation was based on Mori-Tanaka homogenization method and due to the presence of cracks and unpolarized regions in the material, the nominal values of the piezoelectric coefficients had important reductions [16]. Using finite element method, mechanical vibration and bending of FG porous nanobeams were studied by Eltaher et al. The beam was thin and also simply supported. It was presented that, the decrement of the bending resistance and the fundamental frequencies of the beam is obtained by the increase of porosity, nano-scale parameters and material graduation [9].

In this paper, design and analysis of a functionally graded porous piezoelectric cantilever beam is studied and the results are carried out in case of vibrational energy harvesting applications. The structure is composed of a cantilever beam with a proof mass attached to its free vibrating end. By analysing previous investigations and studying the proposed papers in energy harvesting field, it is tried to use the most suitable mathematical modelling procedure in order to obtain more enhanced results.

2. Material properties

According to Fig. 1, it is assumed that the upper surface $\left(z=+h/2\right)$ and the lower surface of the beam $\left(z=-h/2\right)$ are covered with pure aluminium and pure brass, respectively where, the material properties varies smoothly from aluminium to brass through the thickness of the beam (along positive *z* direction). On the other hand, the mixing ratio of these two materials changes smoothly but continuously through the thickness of the microbeam. Hence, it could be assumed that the distribution of these properties through the thickness of the beam follows the linear volume fraction mixing law and is derived from Eq. (1).

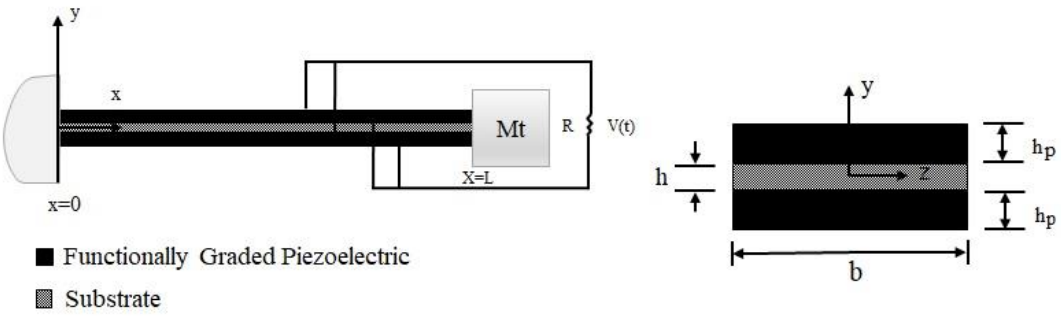

Figure 1. Schematic representation of the bimorph FG porous piezoelectric cantilever beam with a tip mass

$$P = P_{Al}V_{Al}(z) + P_{Br}V_{Br}(z) + \frac{m_0 - m}{m}\left(E_{Al} + E_{Br}\right) \tag{1}$$

In above equation, P_{Al} and P_{Br} represent aluminium and brass surface properties, respectively. Accordingly, V_{Al} and V_{Br} are the upper and lower surfaces aluminium and brass volume fractions, respectively where, in every thickness surface of the beam there is:

$$V_{Al}(z) + V_{Br}(z) = 1, \qquad 0 \le \mathrm{n} \le \infty \tag{2}$$

On the other hand, in Eq. (1), m_0 and m represent beam's mass per unit surface (in the absence of porosity $\beta = 0$) and apparent mass per unit surface (in the presence of porosity $\beta \neq 0$) which are obtained from Eq. (3) and Eq. (4).

$$m_0 = \int_{-h/2}^{+h/2} \rho(z)dz \;|_{\beta=0} \tag{3}$$

$$m = \int_{-h/2}^{+h/2} \rho(z)dz \;|_{\beta\neq0} \tag{4}$$

Using the simple power distribution law, the volume fraction of aluminium part could be described as following:

$$V_{Al}(z) = \left(\frac{z - z_0}{h} + \frac{1}{2}\right)^n, \qquad 0 \le \mathrm{n} \le \infty \tag{5}$$

where, z_0 shows the microbeam's physical neutral plane distance from geometric middle plane, *h* indicates the thickness of the substrate layer and *n* is a non-zero number which represents the power

exponent of functional composition materials. It describes the distribution of material in thickness direction. According to recent assumptions, elastic modulus, mass density and volume fraction of the microbeam could be expressed as [9, 17, 18]:

$$E(z)=\left[E_{Al}-E_{Br}\right]\left(\frac{z-z_0}{h}+\frac{1}{2}\right)^n+E_{Br}+\frac{m_0-m}{m}\left(E_{Al}+E_{Br}\right) \tag{6}$$

$$\rho(z)=\left[\rho_{Al}-\rho_{Br}\right]\left(\frac{z-z_0}{h}+\frac{1}{2}\right)^n+\rho_{Br}+\frac{\beta}{2}\left(\rho_{Al}+\rho_{Br}\right) \tag{7}$$

$$v(z)=\left[v_{Al}-v_{Br}\right]\left(\frac{z-z_0}{h}+\frac{1}{2}\right)^n+v_{Br} \tag{8}$$

Using Eq. (6), the physical neutral plane displacement with respect to the middle plane is:

$$z_0=\frac{\int zE(z)dz}{\int E(z)dz} \tag{9}$$

3. Axial force components and bending moment

Based on the Euler-Bernoulli beam theory, field of displacement of points inside the microbeam in axial and transverse direction could be as below [19]:

$$\begin{Bmatrix}U(x,z,t)\\W(x,z,t)\end{Bmatrix}=\begin{Bmatrix}u(x,z,t)\\w(x,t)\end{Bmatrix}-z\begin{Bmatrix}w_x\\0\end{Bmatrix} \tag{10}$$

where, u and w represent the components of displacement of points on the middle neutral axis in axial and transverse directions in Cartesian coordinates, respectively. According to this theory, it is assumed that the deformation of the beam is only under the influence of bending where, normal lines on beam's transverse sections, before and after deformation, still are perpendicular to the transverse plane.

$$\sigma_{xx}=E(Z)\varepsilon_{xx} \tag{11}$$

Based on recent simplification and by interfering the displacement effect of physical neutral plane with respect to the middle plane, the relation between axial strain and location changes could be as following:

$$\varepsilon_x=u_x+\frac{1}{2}w_x^2-\left(z-z_0\right)w_{xx} \tag{12}$$

where, $\varepsilon_m=u_x+\frac{1}{2}w_x^2-\left(z-z_0\right)w_{xx}$ expresses membrane strains and $\varepsilon_b=-\left(z-z_0\right)w_{xx}$ expresses bending strains. Using Eq. (11) and employing equilibrium equation, the components of axial force and bending moment related to FG microbeam are obtained by integrating over its cross sections.

$$\begin{bmatrix}N_x\\M_x\end{bmatrix}=\int_{-b/2}^{+b/2}\int_{-h/2}^{+h/2}\begin{bmatrix}1\\z-z_0\end{bmatrix}\sigma_x dzdy-\begin{bmatrix}N_x^E\\M_x^E\end{bmatrix} \tag{13}$$

In above equation, by replacing ε_x in Eq. (11) and using Eq. (13), components of axial force and bending moment could be presented in a standard and compressed form as:

$$N_x = A_{11}\varepsilon_m + B_{11}\varepsilon_b - N_x^E \tag{14}$$

$$M_x = B_{11}\varepsilon_m + D_{11}\varepsilon_b - M_x^E \tag{15}$$

where, A_{11}, B_{11} and D_{11} are the axial rigidity, bending and bending-axial coupling coefficients of the beam, respectively which are derived by Eq. (16).

$$\begin{bmatrix} A_{11} \\ B_{11} \\ D_{11} \end{bmatrix} = \int_{-h/2-h_p}^{-h/2} \begin{bmatrix} 1 \\ z - z_0 \\ (z - z_0)^2 \end{bmatrix} E^{piezo} dz + \int_{-h/2}^{+h/2} \begin{bmatrix} 1 \\ z - z_0 \\ (z - z_0)^2 \end{bmatrix} E^{fg}(z) dz + \int_{+h/2}^{+h/2+h_p} \begin{bmatrix} 1 \\ z - z_0 \\ (z - z_0)^2 \end{bmatrix} E^{piezo} dz \tag{16}$$

In Eq. (16), the components of piezoelectric force and moment are achieved by integrating over cross section.

$$\begin{bmatrix} N_{xx}^E \\ M_{xx}^E \end{bmatrix} = -\int_{-h/2-h_p}^{-h/2} e_{31} E_z \begin{bmatrix} 1 \\ z \end{bmatrix} dz - \int_{h/2}^{h/2+h_p} e_{31} E_z \begin{bmatrix} 1 \\ z \end{bmatrix} dz \tag{17}$$

On the other hand, noting that operational piezoelectric layers' thickness is small, the effects of applied potential difference in thickness direction are overcoming the effects of induced potential, so the relation between electrical voltage and created electrical field is as below:

$$E_z = -\frac{v(t)}{h_p} \tag{18}$$

4. The equation of motion of the beam

One of the important variational principles in elastodynamics is Hamilton's principle. Unlike rigid bodies, deformable bodies could have infinite degrees of freedom and also, they can occupy continuous regions of space; consequently, continuous functions of space and time are used to describe the state of the system. Therefore, by the help of Hamilton's principle, nonlinear equations of axial and transverse motions at the points existed on beam's middle plane to the respect of location changes of axial and transverse indices could be obtained as below:

$$A_{11}\frac{\partial^2 u}{\partial x^2} - B_{11}\frac{\partial^3 w}{\partial x^3} + A_{11}\frac{\partial w}{\partial x}\frac{\partial^2 w}{\partial x^2} + \frac{\partial N_x^E(x,t)}{\partial x} - m\frac{\partial^2 u}{\partial t^2} + I_t\frac{\partial^3 w}{\partial x\,\partial t^2} = 0 \tag{19}$$

$$\begin{aligned} &B_{11}\frac{\partial^3 u}{\partial x^3} - D_{11}\frac{\partial^4 w}{\partial x^4} + A_{11}\frac{\partial^2 u}{\partial x^2}\frac{\partial w}{\partial x} + A_{11}\frac{\partial u}{\partial x}\frac{\partial^2 w}{\partial x^2} + \frac{3}{2}A_{11}\left(\frac{\partial w}{\partial x}\right)^2\frac{\partial^2 w}{\partial x^2} - \frac{\partial^2 M_x^E(x,t)}{\partial x^2} + N_x^E(x,t)\frac{\partial^2 w}{\partial x^2} - \\ &c_a\frac{\partial w}{\partial t} - m\frac{\partial^2 w}{\partial t^2} + I_1\frac{\partial^3 u}{\partial x\,\partial t^2} + I_2\frac{\partial^4 w}{\partial x^2\partial t^2} + f(t)\delta(x - L) = 0 \end{aligned} \tag{20}$$

Previous investigations and studies on dynamic/static analysis of functional beams showed that the effect of elastic mode shapes related to lower frequencies are overcoming the higher frequencies mode shapes. So, for studying the transverse shape changing of Euler-Bernoulli beam, Galerkin method is utilized in this paper and one could use some of the first mode shapes in which, satisfies the boundary conditions of edge-bearing support. Also, it helps to transform the dynamic coupled differential equations with partial derivatives to simple nonlinear differential equations. By the recent assumptions, the mechanical coordinate expression is expressed as:

$$w(x) = \sum_{m=1}^{M} q_m(t)\phi_m(x) \tag{21}$$

where, M is the number of semi-waves in axial direction and q_m is the maximum amplitude of shape change related to time in mode shape. Also, ϕ_m is the mass-normalized eigenfunction of the mth vibration mode. In addition to mechanical equations, in vibrational energy harvesting issues, an electrical equation is required, which is derived from the equivalent schematic circuit of the beam. The electrical equation used in this paper, is obtained from [20].

5. Results

The beam is subjected to a proof mass which is 1.82 *gr* and the other end of the beam is fixed. The length and the width of the microbeam are 20 *mm* and 14 *mm*, respectively and the height of the FG piezoelectric layer is 0.06 *mm* and the substrate layer is 0.04 *mm*. Table 1 presents the geometric and material parameters of the system.

Table 1. Geometrical and material parameters

Parameter	Sign	PZT-5A	Brass	Aluminium	Steel
Density (kg.m^{-3})	ρ	7750	9000	2700	7850
Layer's length (mm)	l		20		20
Layer's width (mm)	b		14		14
Layer's height (mm)	h		0.06		0.04
Permittivity constant (nF.m^{-1})	ε_{33}		13.3		
Resistance (Ω)	R		1000		
Volatile fractional composition index	n		0.5		

Fig. 2 shows the output power of the microbeam in the presence of different values of output resistance. According to Ohm's Law, the output resistor adjusts output current and voltage in order to obtain maximum power. It is clear that the power increases sharply with resistance increment until approximately 75 *Kohm*. Then, it decreases slowly with resistance increment. It would be concluded that by placing a 75 *Kohm* resistor at microbeam's output, it could have the maximum output value. Moreover, the power exponent has impacts on the output power, too. The diagram is plotted for 5 different values of power exponent and is shown that, increasing it, will decrease the output power. Furthermore, frequency response plays an important role in microbeam analysis. In this part, the output voltage of the system is studied with frequency changes in the presence of different power exponents. According to Fig. 3, the maximum output voltage is achieved in approximately 220*Hz*

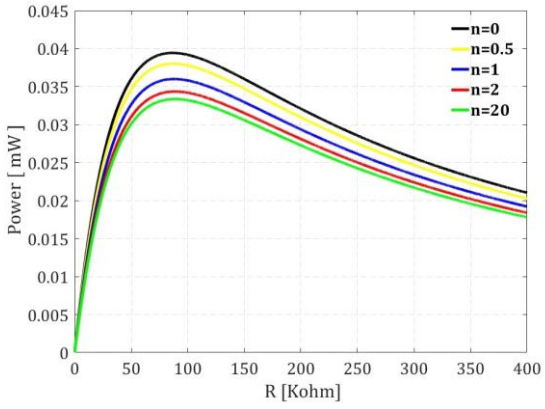

Figure 2. Output power with respect to the resistance for different values of volume fraction index

and it is shown that power exponent increment, decreases output voltage. Finally, it is true that both output power and output voltage decrease with power exponent increment.

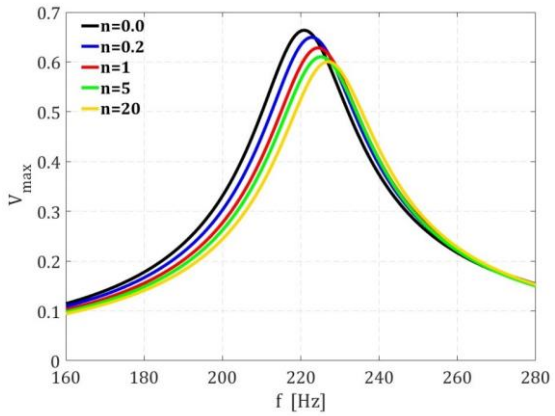

Figure 3. Frequency response of the beam for 5 different values of volume fraction index

Another frequency response analysis could be presented by changing the porosity coefficient. The study shows that the porosity coefficient has impacts on output voltage and increasing it, increases the output voltage, respectively. It is drawn in Fig. 4.

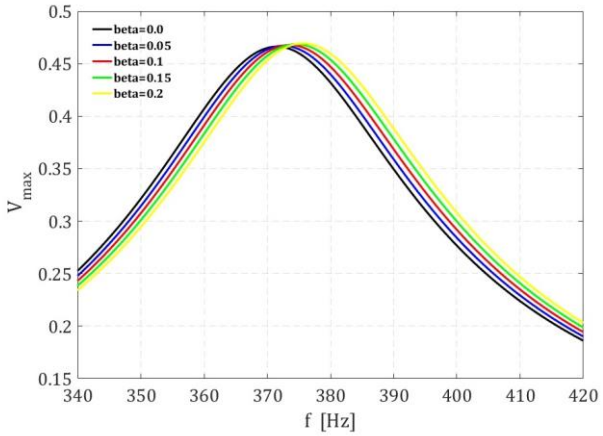

Figure 4. Frequency response of the beam with respect to different values of the porosity coefficients

6. Conclusion

In this paper, a porous FG piezoelectric cantilever beam energy harvester is designed and the mathematical modelling is presented. It has been tried to enhance the efficiency of the energy harvester. Supposing both axial and transverse deformations, the system equations are derived and solved by Galerkin method. Furthermore, three figures are presented which are the most important concerns in such analyses. It is declared that by choosing the best value for the output resistance, the output power would reach its maximum amount. Also, in the presence of FGMs and porosities, there are two significant parameters which are the power exponent and the porosity coefficient. The impact of these parameters is presented in two separate figures. Due to the fact that vibration of a beam has a contrariwise relation with stiffness, it would be concluded from Fig. 2 and 3 that as the characteristics of the FGM changes from aluminum to brass by the increment of power exponent, the stiffness of the beam increases which results in the decrement of both output power and voltage.

REFERENCES

[1] K. Wang, B. Wang, and S. Zeng, "Analysis of an array of flexoelectric layered nanobeams for vibration energy harvesting," *Composite Structures,* vol. 187, pp. 48-57, 2018.

[2] B. Lee, S. Lin, and W. Wu, "Fabrication and evaluation of a MEMS piezoelectric bimorph generator for vibration energy harvesting," *Journal of Mechanics,* vol. 26, no. 4, pp. 493-499, 2010.

[3] M. Majdoub, P. Sharma, and T. Cagin, "Enhanced size-dependent piezoelectricity and elasticity in nanostructures due to the flexoelectric effect," *Physical Review B,* vol. 77, no. 12, p. 125424, 2008.

[4] Y. Zhao, Y. Qin, L. Guo, and B. Tang, "Modeling and experiment of a v-shaped piezoelectric energy harvester," *Shock and Vibration,* vol. 2018, 2018.

[5] C. Cheng, Z. Chen, H. Shi, Z. Liu, and Y. Xiong, "System-Level Coupled Modeling of Piezoelectric Vibration Energy Harvesting Systems by Joint Finite Element and Circuit Analysis," *Shock and Vibration,* vol. 2016, 2016.

[6] X. Li, D. Upadrashta, K. Yu, and Y. Yang, "Sandwich piezoelectric energy harvester: Analytical modeling and experimental validation," *Energy conversion and management,* vol. 176, pp. 69-85, 2018.

[7] Y. Amini, H. Emdad, and M. Farid, "Finite element modeling of functionally graded piezoelectric harvesters," *Composite Structures,* vol. 129, pp. 165-176, 2015.

[8] J. F. Li *et al.*, "Fabrication and evaluation of porous piezoelectric ceramics and porosity–graded piezoelectric actuators," *Journal of the American Ceramic Society,* vol. 86, no. 7, pp. 1094-1098, 2003.

[9] M. Eltaher, N. Fouda, T. El-midany, and A. Sadoun, "Modified porosity model in analysis of functionally graded porous nanobeams," *Journal of the Brazilian Society of Mechanical Sciences and Engineering,* vol. 40, no. 3, p. 141, 2018.

[10] H. A. Atmane, A. Tounsi, and F. Bernard, "Effect of thickness stretching and porosity on mechanical response of a functionally graded beams resting on elastic foundations," *International Journal of Mechanics and Materials in Design,* vol. 13, no. 1, pp. 71-84, 2017.

[11] F. Ebrahimi and M. Zia, "Large amplitude nonlinear vibration analysis of functionally graded Timoshenko beams with porosities," *Acta Astronautica,* vol. 116, pp. 117-125, 2015.

[12] F. Ebrahimi and A. Jafari, "A four-variable refined shear-deformation beam theory for thermo-mechanical vibration analysis of temperature-dependent FGM beams with porosities," *Mechanics of Advanced Materials and Structures,* vol. 25, no. 3, pp. 212-224, 2018.

[13] F. Ebrahimi and A. Dabbagh, "Wave propagation analysis of smart rotating porous heterogeneous piezo-electric nanobeams," *The European Physical Journal Plus,* vol. 132, no. 4, p. 153, 2017.

[14] N. Shafiei, A. Mousavi, and M. Ghadiri, "On size-dependent nonlinear vibration of porous and imperfect functionally graded tapered microbeams," *International Journal of Engineering Science,* vol. 106, pp. 42-56, 2016.

[15] R. Lal and C. Dangi, "Thermal vibrations of temperature-dependent functionally graded non-uniform Timoshenko nanobeam using nonlocal elasticity theory," *Materials Research Express,* vol. 6, no. 7, p. 075016, 2019.

[16] G. Martínez-Ayuso *et al.*, "Model validation of a porous piezoelectric energy harvester using vibration test data," *Vibration,* vol. 1, no. 1, pp. 123-137, 2018.

[17] N. Fouda, T. El-Midany, and A. Sadoun, "Bending, buckling and vibration of a functionally graded porous beam using finite elements," *Journal of Applied and Computational Mechanics,* vol. 3, no. 4, pp. 274-282, 2017.

[18] K. Larkin and A. Abdelkefi, "Neutral axis modeling and effectiveness of functionally graded piezoelectric energy harvesters," *Composite Structures,* vol. 213, pp. 25-36, 2019.

[19] M. Jalaei and Ö. Civalek, "On dynamic instability of magnetically embedded viscoelastic porous FG nanobeam," *International Journal of Engineering Science,* vol. 143, pp. 14-32, 2019.

[20] E. A. Abbasi, A. Allahverdizadeh, R. Jahangiri, and B. Dadashzadeh, "Design and Analysis of a Piezoelectric-Based AC Current Measuring Sensor," *World Academy of Science, Engineering and Technology, International Journal of Mechanical, Aerospace, Industrial, Mechatronic and Manufacturing Engineering,* vol. 11, no. 10, pp. 1661-1666, 2017.